30th International Conference
ENGINEERING MECHANICS 2024
Milovy, Czech Republic, May 14 – 16, 2024

WEAK IMPOSITION OF POTENTIAL DIRICHLET BOUNDARY CONDITIONS IN PIEZOELASTICITY: NUMERICAL STUDY

Cimrman R. *

Abstract: *Detailed modelling of piezoelastic structures often includes also an external circuit. This is tied with the need for a weak imposition of electric potential Dirichlet boundary conditions and questions of simulation accuracy arise. Several methods allowing the weak imposition, namely the non-symmetric Nitsche's method, penalty method and their combinations, are evaluated and their numerical convergence w.r.t. uniform mesh refinement for various finite element approximation orders is reported. The numerical study is performed on a geometry corresponding to a piezoelectric sensor.*

Keywords: Piezoelasticity, Dirichlet boundary conditions, weak imposition, numerical convergence.

1. Introduction

When performing and simulating experiments involving electro-active materials (piezoelectric, flexoelectric, etc.), such as reported in (Cimrman et al., 2023), the electric potential that arises on conductive electrodes is a key quantity to be measured and modeled. The presence of an external circuit (e.g. an oscilloscope) makes the constant potential on an electrode an additional unknown to be computed. As such, the usual potential Dirichlet boundary condition can be enforced only in a weak sense, because its value is not known.

The non-symmetric Nitsche's method without penalty term (Burman, 2012) seemed like a good candidate to be used in combination with the finite element method (FEM), but its slow convergence in our context of 3D piezoelasticity, numerically demonstrated below, motivated this ongoing research of simple and accurate methods for weak application of Dirichlet boundary conditions. We demand a sufficient accuracy even on relatively coarse meshes, because our main interest lies in dynamical simulations.

2. The Finite Element Model

We consider a piezoelastic disc $\Omega \subset \mathbb{R}^3$ whose FEM discretization is shown in Fig. 1. Under linear assumptions, the constitutive relations can be written as

$$\boldsymbol{\sigma} = \boldsymbol{C}^P \boldsymbol{\varepsilon} - \boldsymbol{e}^T \boldsymbol{E} \;, \quad \boldsymbol{d} = \boldsymbol{e}\boldsymbol{\varepsilon} + \boldsymbol{\kappa}\boldsymbol{E} \;, \quad \boldsymbol{\varepsilon} = \frac{1}{2}(\boldsymbol{\nabla}\boldsymbol{u} + \boldsymbol{\nabla}^T\boldsymbol{u}) \;, \quad \boldsymbol{E} = -\boldsymbol{\nabla} p \;, \tag{1}$$

where the mechanical stress $\boldsymbol{\sigma}$ (in Voigt notation vector ordering) and the electric displacement $\boldsymbol{d}$ are proportional to the mechanical strain $\boldsymbol{\varepsilon}$ and the electric field vector $\boldsymbol{E}$, $\boldsymbol{u}$ is the mechanical displacement vector, p the electric potential, $\boldsymbol{C}$ the matrix of elastic properties under constant electric field intensity, $\boldsymbol{e}$ the piezoelectric modulus and $\boldsymbol{\kappa}$ the permittivity under constant deformation. Denoting by Γ_b to bottom and Γ_t the top sides of the disc, where conductive electrodes are situated, the strong form of the problem is: Find p such that

$$\begin{aligned} -\boldsymbol{\nabla}\cdot\boldsymbol{\sigma} = \boldsymbol{b} \text{ in } \Omega \;, \quad \boldsymbol{\nabla}\cdot\boldsymbol{d} = 0 \text{ in } \Omega \;, \\ \boldsymbol{u} = 0 \text{ on } \Gamma_b \;, \quad p = 0 \text{ on } \Gamma_b \;, \quad p = \bar{p} \text{ on } \Gamma_t \;, \end{aligned} \tag{2}$$

* Robert Cimrman: Institute of Thermomechanics of the CAS, Prague & New Technologies - Research Centre and Faculty of Applied Sciences, University of West Bohemia, Plzeň; CZ, cimrman3@ntc.zcu.cz

doi: 10.21495/em2024-078

where $\boldsymbol{b}$ are the self-weight volume forces and $\bar{p}$ is a given potential to be enforced weakly. Zero Neumann boundary conditions are applied on the parts of the Ω boundary not mentioned above.

Let $V_0^u(\Omega) = \{\boldsymbol{u} \in [H^1(\Omega)]^3, \boldsymbol{u} = \boldsymbol{0} \text{ on } \Gamma_b\}$, $V_0^p = \{p \in H^1(\Omega), p = 0 \text{ on } \Gamma_b\}$. The weak form of (2) is then: Find p such that

$$\int_\Omega \boldsymbol{\varepsilon}(\boldsymbol{v})^T \boldsymbol{C} \boldsymbol{\varepsilon}(\boldsymbol{u}) - \int_\Omega \boldsymbol{\varepsilon}(\boldsymbol{v})^T \boldsymbol{e}^T \boldsymbol{\nabla} p - \int_\Omega \boldsymbol{v} \cdot \boldsymbol{b} = 0 \qquad \forall \boldsymbol{v} \in V_0^u(\Omega) \ , \tag{3}$$

$$\int_\Omega (\boldsymbol{\nabla} q)^T \boldsymbol{e} \boldsymbol{\varepsilon}(\boldsymbol{u}) + \int_\Omega (\boldsymbol{\nabla} q)^T \boldsymbol{\kappa} \boldsymbol{\nabla} p - \int_{\Gamma_t} (\boldsymbol{\kappa} \boldsymbol{\nabla} p) \cdot \boldsymbol{n} q = 0 \qquad \forall q \in V_0^p(\Omega) \ , \tag{4}$$

$$\boldsymbol{u} = 0 \ , \quad p = 0 \qquad \text{on } \Gamma_b \ , \tag{5}$$

$$p = \bar{p} \qquad \text{on } \Gamma_t \text{ weakly, see below.} \tag{6}$$

Note that the last term in (4) would be zero if the condition $p = \bar{p}$ on Γ_t was applied as usual by modifying the definition of the test function space V_0^p. The above model is discretized using the FEM, leading formally to the same equations but with functions from appropriate finite element spaces.

3. Weak Imposition of Dirichlet Boundary Conditions

Numerous approaches exist for the weak imposition of Dirichlet boundary conditions, see e.g. (Lu et al., 2019). Here we consider only the non-symmetric (Freund and Stenberg, 1995) Nitsche's method (Nitsche, 1971) with or without penalty term (Burman, 2012). This method introduces additional terms to (4):

$$+ \int_{\Gamma_t} (\boldsymbol{\kappa} \boldsymbol{\nabla} q) \cdot \boldsymbol{n} (p - \bar{p}) + \int_{\Gamma_t} \beta q (p - \bar{p}) \ , \tag{7}$$

where β is the penalty parameter. The pure penalty method can be obtained by omitting the first integral. According to (Babuška, 1973), $\beta = \beta_0 h^{-(2o+1)/3}$, see also (Lu et al., 2019), yields, in the case of the Laplace's problem, for a fixed β_0 the rate of convergence of the order $h^{(2o+1)/3}$ in the energy norm, where h is the element size and o the FE approximation order. For this reason results for the following Laplace's problem (electrostatics)

$$\int_\Omega (\boldsymbol{\nabla} q)^T \boldsymbol{\kappa} \boldsymbol{\nabla} p - \int_{\Gamma_t} (\boldsymbol{\kappa} \boldsymbol{\nabla} p) \cdot \boldsymbol{n} q = 0 \qquad \forall q \in V_0^p(\Omega) \ , \tag{8}$$

$$p = 0 \qquad \text{on } \Gamma_b \ , \tag{9}$$

$$p = \bar{p} \qquad \text{on } \Gamma_t \text{ weakly} \tag{10}$$

are also included in the next section for reference. Again the terms of (7) are added to (8) to enforce (10).

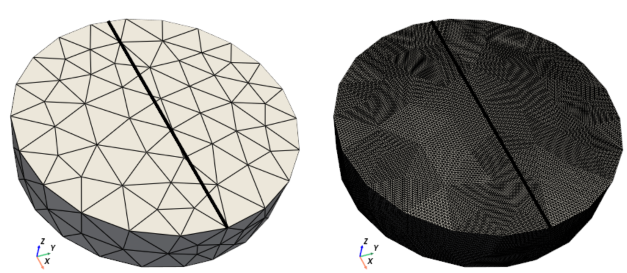

Fig. 1: The FE meshes and probe lines: basic mesh (left), $4\times$ uniformly refined mesh (right).

4. Numerical Convergence Results

The problems specified above were solved for approximation orders $o = \{1, 2, 3\}$ ($\boldsymbol{u}$ and p were approximated with the same order) and uniform mesh refinement levels $r = \{0, 1, 2, 3, 4\}$ with various values of β. The $r = 0$ (152 vertices, 382 elements) and $r = 4$ (280 177 vertices, 1 564 672 elements) meshes can be seen in Fig. 1, together with probe lines along which the $p = \bar{p} = 555$ V satisfaction was checked. The geometry corresponds to a piezoelectric sensor PIC 181 from PI company.

The sensor has the following properties:

$$\text{in Voigt notation: } \boldsymbol{C}^P = \begin{bmatrix} 127.2050 & 80.2122 & 84.6702 & 0.0000 & 0.0000 & 0.0000 \\ 80.2122 & 127.2050 & 84.6702 & 0.0000 & 0.0000 & 0.0000 \\ 84.6702 & 84.6702 & 117.4360 & 0.0000 & 0.0000 & 0.0000 \\ 0.0000 & 0.0000 & 0.0000 & 22.9885 & 0.0000 & 0.0000 \\ 0.0000 & 0.0000 & 0.0000 & 0.0000 & 22.9885 & 0.0000 \\ 0.0000 & 0.0000 & 0.0000 & 0.0000 & 0.0000 & 23.4742 \end{bmatrix} \text{GPa},$$

$$\boldsymbol{e} = \begin{bmatrix} 0.00000 & 0.00000 & 0.0000 & 0.0000 & 17.0345 & 0.0 \\ 0.00000 & 0.00000 & 0.0000 & 17.0345 & 0.0000 & 0.0 \\ -6.62281 & -6.62281 & 23.2403 & 0.0000 & 0.0000 & 0.0 \end{bmatrix} \text{C/m}^2, \boldsymbol{\kappa} = \varepsilon^0 \begin{bmatrix} 1704.4 & 0.0 & 0.0 \\ 0.0 & 1704.4 & 0.0 \\ 0.0 & 0.0 & 1433.6 \end{bmatrix} \text{F/m},$$

where $\varepsilon^0 = 8.8541878128 \cdot 10^{-12}$ F/m is the vacuum permittivity.

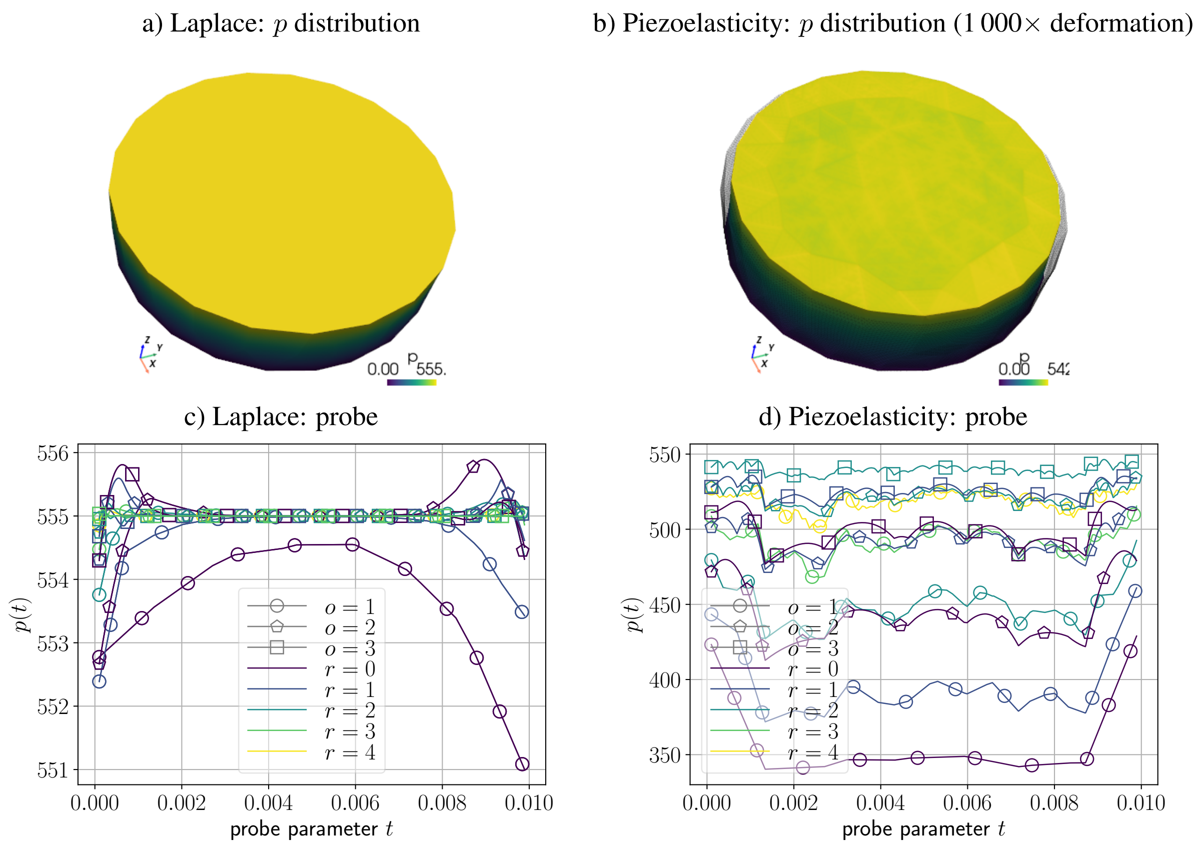

Fig. 2: Nitsche's method without penalty ($\beta = 0$): a) Laplace and b) piezoelasticity distributions of p for $o = 1$ and $r = 4$, c) Laplace and d) piezoelasticity probes of p along the lines in Fig. 1.

All results reported here were obtained using the Open Source finite element software SfePy (Cimrman et al., 2019; Cimrman, 2021). The results for the non-symmetric Nitsche's method without penalty term ($\beta = 0$), our first choice, are illustrated in Fig. 2. While the results for the Laplace's problem (Figs. 2 a) and 2 c) converge relatively well to the prescribed value 555 V, the piezoelasticity problem (Figs. 2 b and 2 d) have low accuracy even for the finest mesh ($r = 4$). Therefore the penalty term was added, either with a constant coefficient $\beta = 1$, or scaled by the local element size $\beta = h^{-(2o+1)/3}$. Overall convergence results are summarized in Fig. 3, where the error is defined as $||p(t) - \bar{p}||_2/N$, $N = 980$ being the fixed number of probe points along the probe line parameterized uniformly by t. The blue $\beta = 0$ lines correspond to the Nitsche's method without the penalty term discussed above. The orange lines show the influence of adding the penalty term, and finally the green dashed lines result from the pure penalty method with $\beta = 1$. When the h scaling of β is used, precision approaching machine limits seem to be reached, however the β values are large: the average values ranged from $5 \cdot 10^2$ ($o = 1$, $r = 0$) up to $2 \cdot 10^8$ ($o = 3$, $r = 3$) — that is significantly higher than in the constant case and it may spoil convergence of iterative solvers due to a bad conditioning of the resulting matrix. The non-scaled $\beta = 1$ curves of the pure penalty method and the Nitsche's method with the penalty visually coincide, which indicates that the effect of the first integral of Eq. (7) is negligible in our setting (compare with the relatively lower accuracy of $\beta = 0$ lines).

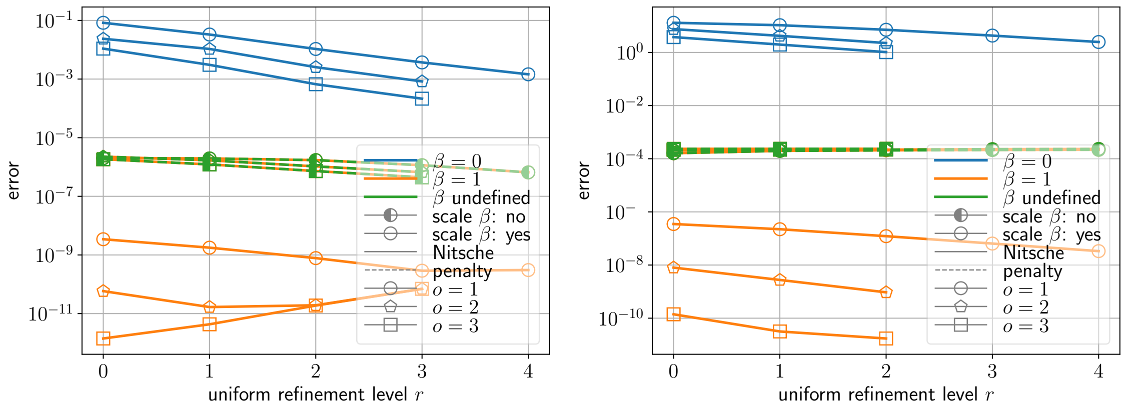

Fig. 3: The h-convergence of the Laplace's (left) and piezoelasticity (right) problems.

5. Conclusion

We have numerically evaluated the Nitsche's and penalty methods for weakly enforcing Dirichlet boundary conditions in the context of piezoelasticity, with the following outcomes. The non-symmetric Nitsche's method without penalty is not accurate enough by itself, only in combination with a penalty. The pure penalty method exhibits a sufficient accuracy even for coarse and low order approximations, although the error does not improve with the increasing order or h-refinement. However this does not present a practical problem in our piezo-elasto-dynamic application, where only second order elements are used to approximate the potential. The problem of bad conditioning with high values of the penalty β can be mitigated by using a direct solver. The influence of adding the Nitsche's method terms to the pure penalty method on the conditioning will be addressed in future.

Acknowledgment

This work has been supported by the grant 23-06220S of the Czech Science Foundation within institutional support RVO:61388998.

References

Babuška, I. (1973) The finite element method with penalty. *Mathematics of Computation*, 27, 122, pp. 221–228.

Burman, E. (2012) A penalty-free nonsymmetric nitsche-type method for the weak imposition of boundary conditions. *SIAM Journal on Numerical Analysis*, 50, 4, pp. 1959–1981.

Cimrman, R. (2021) Fast evaluation of finite element weak forms using Python tensor contraction packages. *Advances in Engineering Software*, 159.

Cimrman, R., Kolman, R., Musil, L., Kotek, V., and Kylar, J. (2023) Dynamics of a cantilever beam with piezoelectric sensor: finite element modeling. In *Proceedings of the 29th International Conference Engineering Mechanics 2023, Milovy, 2023*. pp. 51–54.

Cimrman, R., Lukeš, V., and Rohan, E. (2019) Multiscale finite element calculations in Python using SfePy. *Advances in Computational Mathematics*.

Freund, J. and Stenberg, R. (1995) On weakly imposed boundary conditions for second order problems. *Proceedings of the 9th International Conference on Finite Elements in Fluids*, pp. 327–336.

Lu, K., Augarde, C. E., Coombs, W. M., and Hu, Z. (2019) Weak impositions of dirichlet boundary conditions in solid mechanics: A critique of current approaches and extension to partially prescribed boundaries. *Computer Methods in Applied Mechanics and Engineering*, 348, pp. 632–659.

Nitsche, J. (1971) Über ein Variationsprinzip zur Lösung von Dirichlet-Problemen bei Verwendung von Teilräumen, die keinen Randbedingungen unterworfen sind. *Abhandlungen aus dem Mathematischen Seminar der Universität Hamburg*, 36, 1, pp. 9–15.